11-15-2004

Interfacial Stability of Electrodeposition of Cuprous Oxide Thin Films

Partho Neogi
Missouri University of Science and Technology, neogi@mst.edu

Recommended Citation

P. Neogi, "Interfacial Stability of Electrodeposition of Cuprous Oxide Thin Films," *Journal of Chemical Physics*, American Institute of Physics (AIP), Nov 2004.
The definitive version is available at https://doi.org/10.1063/1.1803541

Interfacial stability of electrodeposition of cuprous oxide films

P. Neogi
Chemical Engineering Department University of Missouri-Rolla Rolla, Missouri 65409-1230

(Received 16 February 2004; accepted 12 August 2004)

Experiments on deposition of Cu_2O films from basic cupper sulfate solution show that copper also deposits. At low, but basic values of *p*H only copper deposits and at high *p*H only cuprous oxide deposits. In the intermediate range where both compete the system shows oscillations at ''constant current.'' Linear stability analysis has been conducted for such an electrochemical cell to show that oscillations can take place in the parameter space identified in the experiments. The results are keeping with most of the experimental observations, which are many, but not with all. The physical mechanisms behind the oscillations are explained in terms of competing reactions. © *2004 American Institute of Physics.* [DOI: 10.1063/1.1803541]

I. INTRODUCTION

Cu_2O has novel electronic properties because of which it is desirable to form a thin film of this material. Switzer and co-workers[1–6] have deposited such films using electrochemical means. Typically, the bath is made by dissolving 90 g of $CuSO_4 \cdot 5H_2O$ in 150 ml of 85% lactic acid and neutralized with 450 ml of 5*M* NaOH. The *p*H is then adjusted to basic value using more of 5*M* NaOH. The electrode reactions were assumed to be

$$Cu^{++} + 2e^- \rightarrow Cu, \tag{1}$$

$$2Cu^{++} + 2OH^- + 2e^- \rightarrow Cu_2O + H_2O. \tag{2}$$

Another reaction is added here for a steady state in the form of

$$2H^+ + 2e^- \rightarrow H_2. \tag{3}$$

It is assumed that hydrogen bubbles at cathode and immediately leaves the solution or that it immediately dissolves in the solution. In either case, it becomes unnecessary to consider Eq. (3) any further in the analysis that follows, and the local concentration of H^+ can be determined by analyzing its solubility product with OH^-. The reaction at anode is assumed to be at the anode

$$Cu \rightarrow Cu^{++} + 2e^-. \tag{4}$$

Their major finding was that a mixture of copper and cuprous oxide was obtained between *p*H of 8.5–10. Below that range of *p*H only metallic copper was obtained, and above that range only cuprous oxide was seen. It is easy to see that the reaction, Eq. (2), is promoted at high *p*Hs. The confounding observation was that in the intermediate values of *p*H, oscillations were observed in the potential at ''constant current.'' The frequency of oscillations increased from about 0.01 Hz to 0.1 Hz with increasing *p*H. Other systems also exist where oscillations have been reported,[7] but the work of Switzer and co-workers is followed here for reasons cited below. They have both in their setup and experimental analysis, considered various factors that could influence the oscillations and followed schemes that are most amenable to modeling. They still leave out many of the rate constants that are needed to fully quantify the oscillations. On varying experimental conditions and characteristics, they could determine no obvious physical/chemical factors which could be held responsible for the oscillations. In this regime, the cathode surface assumes a rough texture, that is, has strong antileveling properties. Exaggerated cases will lead to dendrite formation.[8]

The oscillations at first glance appear sustained, but closer examination shows that the amplitude decreases very slowly with time. Thus, it can be assumed that the response is stable but oscillatory, even though the rate at which the oscillations die is extremely slow. Seshan[9] has shown theoretically that electrodeposition by a single simple reaction such as Eq. (1), is unstable to infinitesimal perturbations, at disturbances of intermediate wavelengths. The analysis first lays out the steady state response and then investigates whether small disturbances grow (unstable) or disappear (stable) in such a system. Since these equations are simplified by linearizing the conservation equations about the base/steady state case, they are a valid description for only the initial development of the disturbances when their amplitudes remain small.[10] Following the procedure in a linear stability analysis, the origin of the disturbances is not tracked. However, the fact that disturbances in all quantities are linked by conservation of mass, etc., is invoked. Miller[11] explains the instability by examining a bump on the cathode as shown in Fig. 1. If the bump arises on the surface of the cathode (where the electrodeposition is taking place), then the length of the path that has to be traversed by the cation to the tip of the bump, that is, the boundary layer, is shorter. Thus the resistance to transport to the tip is smaller, and it would grow faster than the base and develop into dendrite. (See also similar discussion by Johns and Narayanan.[12]) Concentration fluctuations on the surface of the cathode that lead to the formation of the bump, have been measured by Russo *et al.*[13]

Here, Seshan's linear stability analysis has been extended to include the second reaction, Eq. (2), to explore its role on stability and the origin of oscillations. There are significant differences between the system analyzed by Seshan and one considered here. The first of these is the fact that

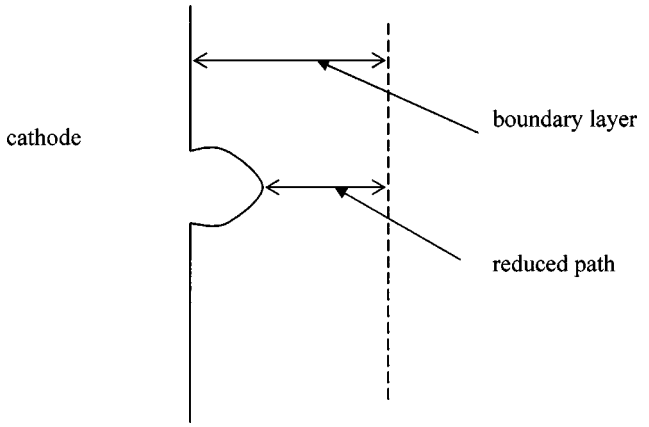

FIG. 1. Basic scheme showing how a bump grows on the cathode.

cuprous oxide has a sizable resistance. A simple model which assumes that the heterogeneous cathode can be represented by one with average properties has been used below to account for its effect on transport. A second feature is that Seshan analyzes only slow modes of growth of disturbances, following similar studies in the formation of dendrites in solidification from melts.[14] However, the oscillations described earlier are comparatively rapid and hence additional terms have to be accounted for in the analysis.

In the sections below, Seshan's model for the electrochemical cell and electrodeposition rates is expanded to include the present system. The effects of perturbations on this system are studied next.

II. BASE CASE

Consider that cathode moves forward into the solution at the rate of V_1 due to the deposit, and due to dissolution, the anode recedes with a velocity V_2 as shown in Fig. 2. It is difficult to work with two separate velocities. Now, a material balance on copper at steady state leads to

$$\left(c_{\mathrm{Cu}}+\frac{2M_{\mathrm{Cu}}}{M_{\mathrm{Cu_2O}}}c_{\mathrm{Cu_2O}}\right)V_1=c^{\circ}_{\mathrm{Cu}}V_2, \tag{5}$$

where the concentrations are in mass, and the cathode is made of copper and cuprous oxide, here assumed to be miscible, or at least that the presence of two separate phases in the cathode need not be separately accounted for. The anode is made of pure copper. Further, $c_{\mathrm{Cu}}=\phi c^{\circ}_{\mathrm{Cu}}$ and $c_{\mathrm{Cu_2O}}=(1-\phi)c^{\circ}_{\mathrm{Cu_2O}}$ in the electrode and superscript (°) denotes pure component and ϕ the volume fraction of copper in the cathode. If the two velocities are equal, then

FIG. 2. Cathode on the left and the anode to the right, moving at unequal rates.

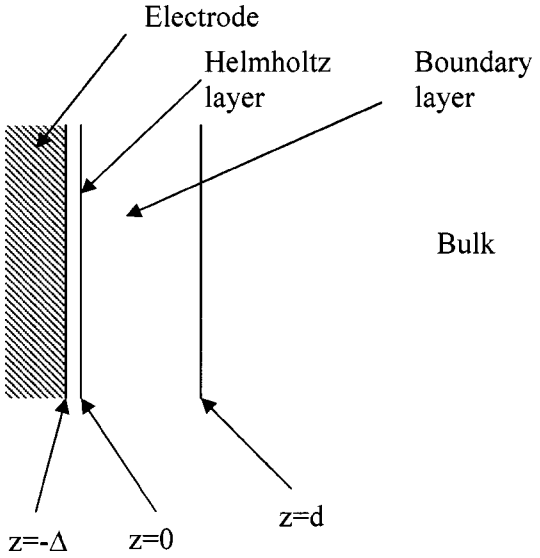

FIG. 3. Dimensions near the cathode are shown. They are similar near the anode. The bulk region finishes at $z=b-d$.

$$\frac{c^{\circ}_{\mathrm{Cu}}}{c^{\circ}_{\mathrm{Cu_2O}}}=2\frac{M_{\mathrm{Cu}}}{M_{\mathrm{Cu_2O}}}. \tag{6}$$

Taking the density of pure copper to be 8.96 g/cm^3 and that of pure cuprous oxide to be 6.0 g/cm^3, the left-hand side is 1.49, and the right-hand side is 1.11. If instead of using separate velocities V_1 and V_2, a single velocity $V=1/2(V_1+V_2)$ is used below. It leads to an error of about 15%, as seen here.

Following Seshan,[9] the electrochemical cell is taken to be well stirred leading to the assumptions that the concentrations and potential there are uniform. The voltage drops/rises only in the Helmholtz layers next to the electrodes where the ionic species under consideration are absent.[15] Between the Helmholtz layers and the well-stirred bulk, lie the unstirred boundary layers, where the concentrations change spatially. Because of very high ionic strengths of the solution in the cell, the electrostatic double layer which lies in this zone is completely suppressed.[16] The coordinate system and locations are shown in one half of the system below in Fig. 3. The bulk of the cell is stirred vigorously, which corresponds to the ''well-stirred'' condition, under which all resistances (to mass transfer and electrical effects) are considered negligible and hence no gradients exist. All resistances lie in the boundary layer of very small thickness (and hence ''unstirred boundary layer'').[17]

III. CONSERVATION OF SPECIES

Steady state equations can be written in moving coordinates in the form of

$$(v_z-V)\frac{dc_i}{dz}=-\frac{d}{dz}j_{zi}. \tag{7}$$

$i=\mathrm{Cu}^{++}$, SO_4^{-}, L^{-} (lactate), Na^{+}, OH^{-}, where the terms on the left determine convection, with v_z as the velocity perpendicular to the cathode, and j_{zi} is the diffusive flux of the ith species. Note that this velocity is not due to stirring, as explained subsequently in detail. Integration leads to

$$(v_z - V)c_i + j_{zi} = \alpha_i, \tag{8}$$

where α_i are the constants of integration. Since $i = SO_4^{--}$, L^- (lactate), Na^+, are nonreactive, their jump mass balance boundary conditions at the cathode leads to

$$(v_z - V)c_i + j_{zi} = 0 \tag{9}$$

that is, their $\alpha_i = 0$. It is very important to note that the convection here in the unstirred boundary layer is not the forced convection that arises due to the stirring in the bulk, it arises out of a change in volume during mass transfer at the interface. Now, if R_1 is rate of consumption of Cu by reaction (1) in mass/(area×time) and R_2 is rate of consumption of Cu by reaction (2) in mass/(area×time) then the remaining jump balances at cathode lead to the following:

For Cu^{++}

$$(v_z - V)c_{Cu^{++}} + j_{zCu^{++}} = -(R_1 + R_2); \tag{10}$$

for OH^-

$$(v_z - V)c_{OH^-} + j_{zOH^-} = -\frac{M_{OH}}{M_{Cu}} R_2; \tag{11}$$

for Cu of volume fraction ϕ in the deposited material

$$-R_1 = (-V)c_{Cu} = (-V)\phi c^\circ_{Cu}; \tag{12}$$

and for Cu_2O

$$-\frac{M_{Cu_2O}}{2M_{Cu}} R_2 = (-V)c_{Cu_2O} = (-V)(1-\phi)c^\circ_{Cu_2O}. \tag{13}$$

Eliminating R_1 and R_2 from Eqs. (10) and (11), by using Eqs. (12) and (13), one has

$$(v_z - V)c_{Cu^{++}} + j_{zCu^{++}} = -V\left[\phi c^\circ_{Cu} + (1-\phi)\frac{2M_{Cu}}{M_{Cu_2O}} c^\circ_{Cu_2O}\right] = -Vc_S, \tag{14}$$

$$(v_z - V)c_{OH^-} + j_{zOH^-} = -V(1-\phi)\frac{2M_{OH}}{M_{Cu_2O}} c^\circ_{Cu_2O} = -Vc_M. \tag{15}$$

Adding Eqs. (14) and (15) as well those for nonreactive species from Eq. (9) (and ignoring the concentration and fluxes for the hydrogen ion in the basic solution)

$$\begin{aligned}(v_z - V)\rho &= -V\left[\phi c^\circ_{Cu} + \frac{(1-\phi)}{M_{Cu_2O}}(2M_{Cu} + 2M_{OH})c^\circ_{Cu_2O}\right] \\ &= -V\left[\phi c^\circ_{Cu} + (1-\phi)\left(1 + \frac{M_{H_2O}}{M_{Cu_2O}}\right)c^\circ_{Cu_2O}\right] \\ &= -Vc_T.\end{aligned} \tag{16}$$

It is possible to use the densities used earlier to calculate $c_T = \phi 8.96 + (1-\phi)(1 + 18/143.1)6 = 8.96\phi + 5.25(1-\phi)$ in g/cm^3, $c_M = (1-\phi)0.238$ g/cm^3, and $c_S \approx c_T$. The bulk concentrations given earlier lead to (approximately) $\rho = 0.545$ g/cm^3 for the total mass concentration of all ions. It is assumed to be a constant. Note that Eq. (16) is a mass jump balance: the total mass moving from the liquid phase to the interface is being equated to the total mass that has moved from the interface into the electrode. For the particular case where $\rho = c_T$, $v_z = 0$ for all values of V, that is, convection does not arise when there is a density match.

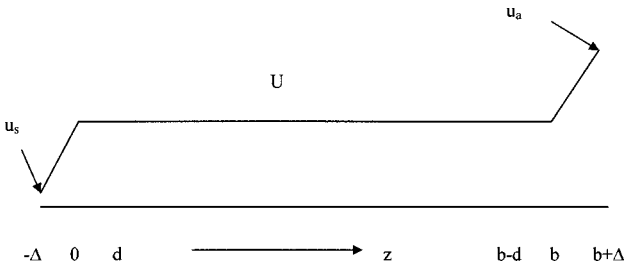

FIG. 4. Model electric potential profile in the cell.

Eliminating $(v_z - V)$ using Eq. (16), and taking into account that the electrolyte concentration is large that the double layers are suppressed then the diffusive fluxes are

$$j_{zi} = -D_i \frac{dc_i}{dz}, \tag{17}$$

the concentrations of the reactive species work out on integration to be

$$c_{Cu^{++}} = \frac{\rho c_S}{c_T} + \beta_{Cu^{++}} e^{Vc_T z/\rho D_{Cu^{++}}}, \tag{18}$$

$$c_{OH^-} = \frac{\rho c_M}{c_T} + \beta_{OH^-} e^{Vc_T z/\rho D_{OH^-}}. \tag{19}$$

Bulk concentrations (subscript b) are known, and using these for boundary conditions, one has on the cathode side

$$c_i = c_{ib} e^{[Vc_T(z-d)/\rho D_i]} \tag{20}$$

for $i = Na^+$, L^-, SO_4^{--}, where d is the thickness of the boundary layer: see Fig. 3. In addition,

$$c_{Cu^{++}} = \frac{\rho c_S}{c_T} + \left[c_{Cu^{++}b} - \frac{\rho c_S}{c_T}\right] e^{[Vc_T(z-d)/\rho D_{Cu^{++}}]}, \tag{21}$$

$$c_{OH^-} = \frac{\rho c_M}{c_T} + \left[c_{OH^-b} - \frac{\rho c_M}{c_T}\right] e^{[Vc_T(z-d)/\rho D_{OH^-}]}, \tag{22}$$

and on the anode side

$$c_i = c_{ib} e^{[Vc_T(z-b+d)/\rho D_i]} \tag{23}$$

for $i = Na^+$, L^-, SO_4^{--}. Here, b is the distance between two electrodes (see Fig. 4). Further,

$$c_{Cu^{++}} = \frac{\rho c_S}{c_T} + \left[c_{Cu^{++}b} - \frac{\rho c_S}{c_T}\right] e^{[Vc_T(z-b+d)/\rho D_{Cu^{++}}]}, \tag{24}$$

$$c_{OH^-} = \frac{\rho c_M}{c_T} + \left[c_{OH^-b} - \frac{\rho c_M}{c_T}\right] e^{[Vc_T(z-b+d)/\rho D_{OH^-}]}. \tag{25}$$

Solutions to Laplace equation for the two dimensionless potentials in the Helmholtz layers, are explained in Fig. 4. Near cathode, the potential is u_H

$$u_H = \frac{U-u_s}{\Delta} z + U, \tag{26}$$

where $u_s = \psi(1-\phi)$. Here u_s cuts down the net potential difference by an amount proportional to the volume fraction of the deposited cuprous oxide, which is the model used here to include the electrical resistance of the deposited cuprous oxide. In particular, for a cathode of pure copper the potential would be zero, and ψ for a cathode of pure cuprous oxide. As shown in Fig. 4, it increases the potential at the cathode from zero for pure copper, to u_s. Near the anode the potential is u'_H,

$$u'_H = \frac{u_a - U}{\Delta} z + U\left(1 + \frac{b}{\Delta}\right) - u_a \frac{b}{\Delta}. \tag{27}$$

All terms in u and U are dimensionless potentials, made dimensionless by multiplying with F/RT where F is a Faraday.

In summary, the exact representation in the boundary layer requires the use of Nernst–Planck equation for the fluxes which includes the effect of the potential gradient, and not the Fick's laws. The potential itself is governed by Poisson equation. However, in the problem under consideration, the ionic strength is very high which leads to negligible charge density when Poisson equation is properly scaled, even though the concentrations of all ions vary inside the boundary layer. In this case of negligible charge density, the above Poisson equation becomes Laplace equation. The solution to Laplace equation in one dimension is one with constant gradient of electric potential, that is, constant field. This constant value has to be equal to that in the bulk at the boundary layer—bulk interface. As the value of the gradient in the well-stirred bulk is zero and there is no charge accumulation at the above interface, the potential gradient in the boundary layer is zero as shown in Fig. 4. Consequently, the Nernst–Planck equation for fluxes become Fick's law, Eq. (17).

IV. REACTION KINETICS

Substituting elementary reaction models for R_1 and R_2 into Eqs. (12) and (13) and taking the anodic reactions there to be given by Eq. (4), one has

$$V\phi c^\circ_{Cu} = k_{c_1} c_{Cu^{++}} e^{\beta(U-u_s)} - k_{a_1} \phi c^\circ_{Cu} e^{-(1-\beta)(U-u_s)} \tag{28}$$

at $z=0$, which becomes on nondimensionalization

$$\mathrm{Pe}\phi = D_{a1}\theta_{Cu^{++}}(0) e^{\beta(U-u_s)} - D'_{a1}\phi e^{-(1-\beta)(U-u_s)}, \tag{29}$$

where the Peclet number $\mathrm{Pe} = Vd/D_{Cu^{++}}$ and the two Damkohler numbers are $D_{a1} = k_{c1} c_{Cu^{++}b} d/D_{Cu^{++}} c^\circ_{Cu}$, and $D'_{a1} = k_{a1} d/D_{Cu^{++}}$. The dimensionless Peclet number Pe, is the ratio between convection and diffusion, and Damkohler numbers are ratios between reaction and diffusion. In addition, $\theta_i = c_i/c_{ib}$ and β, the transfer coefficient, is an empirical constant ~ 0.5. Similarly, for the second reaction

$$V(1-\phi)c^\circ_{Cu} = \frac{M_{Cu_2O}}{2M_{Cu}}\left[k_{c2} c^2_{Cu^{++}}(0) c^2_{OH^-}(0) e^{\beta(U-u_s)} - k'_{a_1}\phi c^\circ_{Cu} e^{-(1-\beta)(U-u_a)}\right], \tag{30}$$

$$\mathrm{Pe}(1-\phi)\frac{2M_{Cu}}{M_{Cu_2O}} = D_{a2}\theta^2_{Cu^{++}}(0)\,\theta^2_{OH^-}(0) e^{\beta(U-u_s)} - D'_{a1}\phi e^{-(1-\beta)(U-u_a)}, \tag{31}$$

where it has been assumed in Eq. (31) that $k'_{a1} = k_{a1}$ and $D_{a2} = k_{c2} c^2_{Cu^{++}b} c^2_{OH^-b} d/D_{Cu^{++}} c^\circ_{Cu}$. Further, for the reaction at the anode

$$Vc^\circ_{Cu} = -k^*_{c_1} c_{Cu^{++}}(b) e^{-\beta(u_a-U)} + k^*_{a1} c^\circ_{Cu} e^{(1-\beta)(u_a-U)}, \tag{32}$$

$$\mathrm{Pe} = -D_{a1}\theta_{Cu^{++}}(b) e^{-\beta(u_a-U)} + D'_{a1} e^{(1-\beta)(u_a-U)}, \tag{33}$$

where it has been assumed in Eq. (33) that $k^*_{a1} = k_{a1}$ and $k^*_{c1} = k_{c1}$. The dimensionless concentrations at the electrodes become

$$\theta_{Cu^{++}}(0) = \frac{\rho c_S}{c_{Cu^{++}b} c_T} + \left[1 - \frac{\rho c_S}{c_{Cu^{++}b} c_T}\right] e^{\mathrm{Pe} c_T/\rho}, \tag{34}$$

$$\theta_{OH^-}(0) = \frac{\rho c_M}{c_{OH^-b} c_T} + \left[1 - \frac{\rho c_M}{c_{OH^-b} c_T}\right] e^{\mathrm{Pe} c_T D_{Cu^{++}}/\rho D_{OH^-}}, \tag{35}$$

$$\theta_{Cu^{++}}(b) = \frac{\rho c_S}{c_{Cu^{++}b} c_T} + \left[1 - \frac{\rho c_S}{c_{Cu^{++}b} c_T}\right] e^{-\mathrm{Pe} c_T/\rho}. \tag{36}$$

Since ρ is much higher than any of the other concentrations in Eqs. (34)–(36), Pe will have to be very small. If $\mathrm{Pe}=0$ (that is, vanishingly small), the reaction limiting case arises since then the concentrations of the reactive species become uniform in the boundary layer. Eqs. (29), (31), (33) can be solved subject to (34)–(36), to obtain Pe, U, and ϕ. These equations have been solved exhaustively by Seshan[9] for the case where the second reaction at the cathode is missing (and hence, $\phi=1$). Here, Eq. (33), which can be used to evaluate u_a, has been ignored. Equations (29) and (31) can be used to calculate the values of D_{a1} and D_{a2} for given values of Pe, U, and ϕ.

Some features of the basic model are emphasized. As mentioned earlier, elementary kinetics has been used to write the rates of reactions. This is often a simplification.[18,15] The manner in which copper ions pass through different oxidation states is known to be nontrivial.[19] Further, the issues raised by Erné *et al.*[7] can be extrapolated to here to point out one simplification in the present model. The surface voltage on the cathode on the oxide patch will be higher than u_s and that on the metal will be lower than u_s. It is assumed here that these differences can be ignored and the average voltage u_s can be used. In turn, it leads to the assumption that R_1 and R_2 are not too different on the oxide patches than on the metal for the averaging to be meaningful. These differences will arise since the magnitudes of R_1 and R_2 depend on the surface potentials. Additionally, it needs to be assumed that the present analysis is confined to initial times such that the differences in R_1 and R_2 on oxide patches, do not by them-

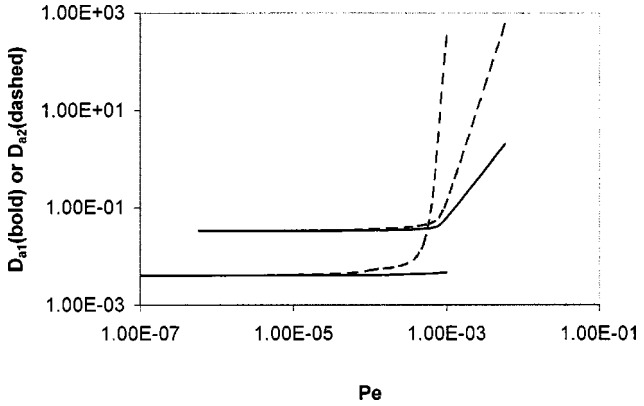

FIG. 5. The two Damkohler numbers D_{a1} (bold line) and D_{a2} (dashed line) are plotted against Pe using Eqs. (29), (31), (34) and (35). $D'_{a1}=0.1$, $\psi=0.1$, and $\beta=0.5$. The top set is for $\phi=0.9$ and the bottom set is for $\phi=0.1$. $U=1$ for both sets.

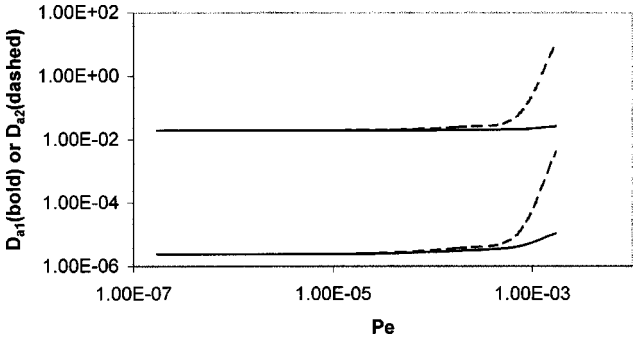

FIG. 6. The two Damkohler numbers D_{a1} (bold line) and D_{a2} (dashed line) are plotted against Pe using Eqs. (29), (31), (34), and (35). $D'_{a1}=0.1$, $\psi=0.1$, and $\beta=0.5$. The top set is for $U=1$ and the bottom set is for $U=100$. $\phi=0.5$ for both sets.

selves lead to a significantly bumpy surface. The oscillations are seen to start initially so that this assumption is justified. Given the many variations and complications that can arise, it seems quite reasonable to work with averages, even though this make lead to a very simplified reaction scheme.

V. PERTURBATIONS

All perturbed quantities are shown with subscript (p) and are proportional to $e^{i\omega x}e^{\mathrm{Bt}}$. These are

$$\frac{\partial^2 u_p}{\partial z^2}+\frac{\partial^2 u_p}{\partial x^2}=0, \tag{40}$$

$$u_p|_{z=-\Delta}+\left.\frac{\partial u}{\partial z}\right|_{z=-\Delta}=u_{sp}=-\phi_p\psi, \tag{41}$$

$$u_p|_{z=-\Delta}+\frac{U-(1-\phi)\psi}{\Delta}\Lambda=u_{sp}=-\phi_p\psi, \tag{42}$$

$$u_p|_{z=0}+\frac{U-(1-\phi)\psi}{\Delta}\Lambda=0. \tag{43}$$

Let $u_p=A(z)e^{i\omega x}e^{\mathrm{Bt}}$, then

$$A=a\cos(\omega z)+b\sin(\omega z). \tag{44}$$

If in addition, the perturbation to the location of the outer Helmholtz plane at the cathode is $\Lambda=ce^{i\omega x}$ and that to the concentration of the deposited copper is $\phi_p=\delta e^{i\omega x}$, one has

$$a=-\frac{U-u_s}{\Delta}c \tag{45}$$

$$a\cos(\omega\Delta)-b\sin(\omega\Delta)-a=\delta\psi. \tag{46}$$

It is now possible to consider the equations of conservation of species. Mullins and Sekerka[14] ignored both the unsteady state terms and the convective terms in their analysis. These assumptions were also made by Seshan,[9] and are enough to predict dendrite formation. These are slow modes and such assumptions are retained for only the non-reactive species $i=\mathrm{L}^-$, Na^+, SO_4^-, leading to

$$\frac{\partial^2 c_{ip}}{\partial z^2}+\frac{\partial^2 c_{ip}}{\partial x^2}=0, \tag{47}$$

$$-D_i\frac{\partial c_{ip}}{\partial z}=0 \quad \text{at } z=0, \tag{48}$$

$$c_{ip}=0 \quad \text{at } z=d. \tag{49}$$

The solution is

$$c_{ip}=0. \tag{50}$$

For the reactive species Cu^{++} and OH^- some effort is made to keep both those terms since the oscillations are a lot faster than the basic growth. This leads to

$$\frac{\partial c_{ip}}{\partial t}+(v_{zp}-V_p)\frac{\partial c_i}{\partial z}=D_i\left[\frac{\partial^2 c_{ip}}{\partial x^2}+\frac{\partial^2 c_{ip}}{\partial z^2}\right], \tag{51}$$

where a term $(v_z-V)\partial c_{ip}/\partial z$ has been neglected as it is a product of two small terms. By perturbing Eq. (16) one obtains $(v_{zp}-V_p)\approx -V_p(c_{\mathrm{T}}/\rho)$, where a few terms have been ignored under the same assumption as above, viz., velocities are small and the terms containing velocities can be ignored when they are multiplied with small (perturbed) concentration. That is, the terms neglected are smaller than the perturbations by a factor of the order of Peclet number Pe, which is 10^{-2} or far less as shown in Figs. 5 and 6. One boundary condition is still Eq. (49), the other is simply perturbations of Eqs. (14) and (15)

$$-V_p\frac{c_{\mathrm{T}}}{\rho}c_{\mathrm{Cu}^{++}}-D_{\mathrm{Cu}^{++}}\frac{\partial c_{\mathrm{Cu}^{++}p}}{\partial z}=-V_pc_s-V\phi_p\left[c^{\circ}_{\mathrm{Cu}^{++}}-\frac{2M_{\mathrm{Cu}}}{M_{\mathrm{Cu_2O}}}c^{\circ}_{\mathrm{Cu_2O}}\right], \tag{52}$$

$$-V_p\frac{c_{\mathrm{T}}}{\rho}c_{\mathrm{OH}^-}-D_{\mathrm{OH}^-}\frac{\partial c_{\mathrm{OH}^-p}}{\partial z}=-V_pc_{\mathrm{M}}-V\phi_p\frac{2M_{\mathrm{OH}}}{M_{\mathrm{Cu_2O}}}c^{\circ}_{\mathrm{Cu_2O}}. \tag{53}$$

The solution is

$$c_{ip}=f_i\sinh(y_iz)+g_i\cosh(y_iz)+\frac{c_{\mathrm{T}}}{\rho}\frac{\hat{V}_p}{D_iy_i^2}\frac{\partial c_i}{\partial z}, \tag{54}$$

assuming that the fluctuations take place over a much small length scale than the base gradient. Here,

$$g_i = -f_i \tanh(y_i d) - \frac{\hat{V}_p c_T}{\cosh(\Omega_i)\rho D_i y_i^2}\frac{\partial c_T}{\partial z}$$

and

$$y_i^2 = \omega^2 + B/D_i .$$

Further,

$$f_{Cu^{++}} = \frac{\hat{V}_p[c_S - c_T c_{Cu^{++}}(0)/\rho]}{y_{Cu^{++}} D_{Cu^{++}}}, \tag{55}$$

$$f_{OH^-} = \frac{\hat{V}_p[c_M - c_T c_{OH^-}(0)/\rho] - V\delta\left[\frac{2M_{OH}}{M_{Cu_2O}} c^{\circ}_{Cu_2O}\right]}{y_{OH^-} D_{OH^-}}, \tag{56}$$

where $V_p = \hat{V}_p e^{i\omega x} e^{Bt}$, $\phi_p = \delta e^{i\omega x} e^{Bt}$ and the perturbation to the thickness of the deposit on cathode is $\Lambda = c e^{i\omega x} e^{Bt}$. It also follows that as $V_p = \partial\Lambda/\partial t$, $\hat{V}_p = Bc$. For perturbations with small amplitudes the reaction boundary conditions become simply perturbations of Eqs. (14) and (15). That for Eq. (14) is

$$V_p \phi c^{\circ}_{Cu} + V\phi_p c^{\circ}_{Cu} = R_{1p} . \tag{57}$$

Perturbing the rate expression from the right-hand side of Eq. (28) to substitute into the right-hand side in Eq. (57) using the above expression for small changes in velocity of the front and deposit thicknesses, and then nondimensionalizing, one has

$$\begin{aligned}
&\frac{c}{d}\tilde{B}\Bigg[\phi + D_{a1}\frac{[c_S - c_T c_{Cu^{++}}(0)/\rho]}{c_{Cu^{++}b}}\frac{\tanh(\Omega_{Cu^{++}})}{\Omega_{Cu^{++}}}e^{\beta\Delta u} \\
&\quad + \frac{D_{a1}}{\Omega^2_{Cu^{++}}}\frac{c_T}{\rho}\frac{\partial\theta_{Cu^{++}}}{\partial\zeta}(0)(\operatorname{sech}\Omega_{Cu^{++}} - 1)e^{\beta\Delta u}\Bigg] \\
&= \frac{c}{d}\Bigg[D_{a1}\frac{\partial\theta_{Cu^{++}}}{\partial\zeta}(0)e^{\beta\Delta u} + D_{a1}\theta_{Cu^{++}}(0)\beta\frac{\partial u}{\partial\zeta}(0)e^{\beta\Delta u} \\
&\quad + D'_{a1}\phi(1-\beta)\frac{\partial u}{\partial\zeta}(0)e^{-(1-\beta)\Delta u}\Bigg] \\
&\quad + \delta[-\mathrm{Pe} + D_{a1}\theta_{Cu^{++}}(0)\beta\psi e^{\beta\Delta u} - D'_{a1}e^{-(1-\beta)\Delta u} \\
&\quad + D'_{a1}\phi(1-\beta)\psi e^{-(1-\beta)\Delta u}],
\end{aligned} \tag{58}$$

where $\Omega_i = y_i d$, $\Delta u = U - u_s$, $\zeta = z/d$, and $\tilde{B} = Bd^2/D_{Cu^{++}}$. Perturbing Eq. (15) leads to

$$V_p(1-\phi)c^{\circ}_{Cu} - V\phi_p c^{\circ}_{Cu} = R_{2p} \tag{59}$$

and eventually to

$$\begin{aligned}
&\frac{c}{d}\tilde{B}\Bigg[(1-\phi) + \frac{D_{a2}}{\Omega^2_{Cu^{++}}}\frac{c_T}{\rho}\frac{\partial\theta_{Cu^{++}}}{\partial\zeta}(0)(\operatorname{sech}\Omega_{Cu^{++}} - 1)2\theta_{Cu^{++}}(0)\theta^2_{OH^-}(0)e^{\beta(U-u_s)} \\
&\quad + \frac{D_{a2}\tan(\Omega_{Cu^{++}})}{\Omega_{Cu^{++}}}\frac{[c_S - c_T c_{Cu^{++}}(0)/\rho]}{c_{Cu^{++}b}}2\theta_{Cu^{++}}(0)\theta^2_{OH^-}(0)e^{\beta(U-u_s)} + \frac{D_{a2}\tan(\Omega_{OH^-})}{\Omega_{OH^-}}\frac{[c_M - c_T c_{OH^-}(0)/\rho]}{c_{OH^-b}} \\
&\quad \times 2\theta^2_{Cu^{++}}(0)\theta_{OH^-}(0)e^{\beta(U-u_s)} + \frac{D_{a2}}{\Omega^2_{OH^-}}\frac{c_T}{\rho}\frac{\partial\theta_{OH^-}}{\partial\zeta}(0)(\operatorname{sech}\Omega_{OH^-} - 1)2\theta^2_{Cu^{++}}(0)\theta_{OH^-}(0)e^{\beta(U-u_s)}\Bigg] \\
&= \frac{c}{d}\Bigg[D_{a2}\frac{\partial}{\partial\zeta}(\theta^2_{Cu^{++}}\theta^2_{OH^-})(0)e^{\beta(U-u_s)} + D_{a2}(\theta^2_{Cu^{++}}\theta^2_{OH^-})(0)\beta\frac{\partial u}{\partial\zeta}(0)e^{\beta(U-u_s)} + D'_{a1}(1-\phi) \\
&\quad \times(1-\beta)\frac{\partial u}{\partial\zeta}(0)e^{-(1-\beta)(U-u_s)}\Bigg] + \delta\Bigg[\mathrm{Pe} + D_{a2}\theta^2_{Cu^{+-}}(0)\theta^2_{OH^-}(0)\beta\psi e^{\beta(U-u_s)} - D'_{a1}e^{-(1-\beta)(U-u_s)} \\
&\quad + D'_{a1}(1-\phi)(1-\beta)\psi e^{-(1-\beta)(U-u_s)} + D_{a2}\frac{D_{Cu^{++}}}{D_{OH^-}}2\theta^2_{Cu^{++}}(0)\theta_{OH^-}(0)\frac{\tan(\Omega_{OH^-})}{\Omega_{OH^-}}\mathrm{Pe}\frac{2M_{OH}}{M_{Cu_2O}}e^{\beta(U-u_s)}\Bigg].
\end{aligned} \tag{60}$$

The unknowns c/d and δ can be eliminated from Eqs. (58) and (60), leaving one with the dispersion equation in the form of B as a function of ω. Concentration profiles are available in Eqs. (21) and (22). In addition, $\partial u/\partial\zeta(0) = \Delta u$.

An important comment to make here is that such results assume that the constant current control system is fully ineffective in eliminating current fluctuations. It is also possible to assume that it is fully effective. In the latter case, the fluctuating current can be set to zero, which gives us a relation between c/d and δ. Substituting for c/d into Eqs. (58) and (60), two solutions for δ as a function of B and α. Equating the two results leads to B as a function of α. Intermediate cases require the knowledge of the control system. It is more

reasonable to assume that the control system is ineffective particularly for disturbances of high frequency considered here.

VI. RESULTS AND DISCUSSION

The steady responses are shown in Figs. 5 and 6. In Fig. 5, the smaller values of Pe represent the region which is reaction controlled, as mentioned earlier. In the region of large Pe, as the system is diffusion limited, the reaction rates are quantified by the Damkohler numbers, D_{a2} and D_{a1}, which are observed to be very high. The values of concentration of OH^- ions at the cathode fall towards zero with increasing Pe in this domain, since the second reaction which consumes this ion becomes overpowering. Starting from the left, Pe is stopped abruptly at a point where this concentration reaches zero. This value of Pe is only a little below Pe, max, the smallest value of Pe at which one of the two reactants reach zero concentration at the cathode, usually OH^-. The values of D_{a2} increase (far more than that for D_{a1}) as Pe increases and seem to go towards infinity near Pe, max. Two sets of values of ϕ have been used here. The values of Damkohler numbers obtained for $\phi=0.9$ are at least one order of magnitude larger than those for $\phi=0.1$. This happens as the first reaction, Eq. (1), that deposits copper, appears to be reaction controlled in general. Hence, higher D_{a1} implies higher copper. Similar trends are seen in Fig. 6, where an intermediate value of $\phi=0.5$ but two different values of U have been used. Higher values of U increase the effective values the Damkohler numbers and hence their actual values are a lot lower. The key feature of Figs. 5 and 6, it should be emphasized, is that the first reaction is reaction controlled or very close. Other constants were chosen to be $D'_{a1}=0.1$ and $\psi=0.1$ throughout. In addition, it was assumed that $D_{Cu^{++}} \approx D_{OH^-}$.

The stability results are analyzed next. Homogeneous equations, Eqs. (58) and (60), admit a solution only if the determinant of their coefficient matrix is zero. This leads to an equation for the dimensionless rate of growth $\tilde{B}$ as function of the dimensionless wave number ωd. When B is complex, the system oscillates, and it is stable or unstable according to whether the real part of B is negative or positive. One important part is missing. The effect of surface tension on the electrode surface, which has been included by Seshan,[8] has been left out here for simplicity. It is well known that this effect is very important at disturbances of small wavelengths because large surfaces areas are produced. Surface tension acts to reduce this by eliminating these perturbations. Consequently, Seshan's result that the surface tension stabilizes disturbances of small wavelengths (large wave numbers ω) is taken here for granted, and attention is focused on disturbances of large wavelengths (small ω).

Some simplifying assumptions are made. The terms in D'_{a1} are ignored as very small. Ω is assumed to be small, that is, $\tanh(\Omega)/\Omega \approx 1-\Omega^2/3$ and $(\operatorname{sech}\Omega-1)/\Omega^2 \approx -1/2+5\Omega^2/24$, where for small values of ωd here, $\Omega^2 \approx \tilde{B}$. Further, the first reaction is assumed to be always reaction controlled, that is, $\theta_{Cu^{++}}(0)\approx 1$, $\partial\theta_{Cu^{++}}/\partial\zeta(0)\approx 0$. For the second reaction, it is possible to have the following.

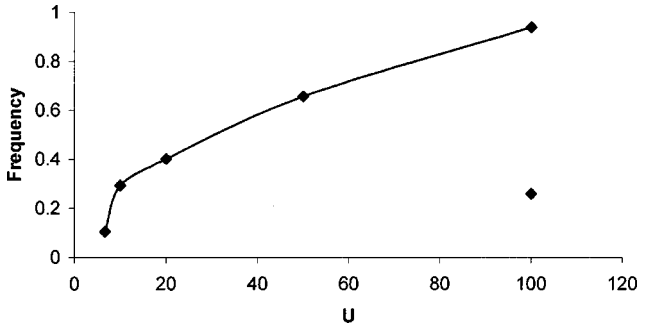

FIG. 7. The absolute value of the imaginary part of $\tilde{B}$, which is the dimensionless frequency, is plotted against U. The values are all for $\phi=0.3$, Pe $=0.001\,29$. The curve is for small $\tilde{B}$ approximation and the solitary point is for large $\tilde{B}$ approximation. These are all from diffusion controlled region.

(a) Reaction controlled: In this case Pe is small as well and $\theta_{OH^-}(0)\approx 1$, $\partial\theta_{OH^-}/\partial\zeta(0)\approx(1-0)/1=0$. The simplifications lead to an involved quadratic equation in $\tilde{B}$.

(b) Diffusion controlled: Here Pe is large, and $\theta_{OH^-}(0)\approx 0$ and $\partial\theta_{OH^-}/\partial\zeta(0)\approx 1$. However, in this form most terms disappear.

Instead, the approximation that $2\theta_{OH^-}(0)\partial\theta_{OH^-}/\partial\zeta(0) = \partial\theta^2_{OH^-}/\partial\zeta(0)\approx(1-0)/1=1$, is used since this is how the terms on the far left had originated in the first place. Again, a quadratic equation in $\tilde{B}$ is obtained. $\tilde{B}$ is found to be real and positive in almost all cases except in a few, where $\tilde{B}$ is complex. These occur at large values of Pe, as appropriate for the diffusion limited case. It only occurs at $\phi=0.3$.

It is also necessary to find approximations that focus on large values of $\tilde{B}$, in particular, because the right-hand side in Eq. (51) was introduced to accommodate this case. Here, $\tanh(\Omega)/\Omega \sim 1/\Omega$ and $[\operatorname{sech}(\Omega)-1]/\Omega^2 \sim -1/\Omega^2$ and $\Omega^2 \approx \tilde{B}$ as before. These approximations lead to quadratic equations in $\tilde{B}^{1/2}$ for both cases of (a) reaction controlled and (b) diffusion controlled.

The parameter space searched was $\phi=0.1$, 0.3, 0.5, 0.7, 0.9, and $U=0$, 1, 3.33, 6.67, 10, 20, 50, and 100. The Pe values were taken up in five steps of a factor of 10 up to a little less that Pe,max for that value of ϕ. Barring the complex roots of $\tilde{B}$, all other roots were found to be real with one or both roots positive, that is, the system is unstable. The absolute value of the imaginary part of the complex root is called frequency in Figs. 7 and 8. The approximate results from the diffusion controlled regime are shown in Fig. 7. All values are for $\phi=0.3$ and $\mathrm{Pe}=0.001\,29$ only. No other complex roots were found in this domain of large Pe. The curve was obtained for the small $\tilde{B}$ approximation, and the solitary point for the large $\tilde{B}$ approximation.

Figure 8 contains all the complex roots found in the reaction controlled regime. None were found in the large $\tilde{B}$ approximation. The upper line is for $\phi=0.7$ and the lower line is for $\phi=0.9$. The larger frequencies are for $U=6.67$ and the smaller ones are for $U=10$.

All frequencies are in the range of where oscillations have been observed experimentally. However, the cases where computations show oscillations are sparse, and it is very likely that the piecemeal approximations used here do

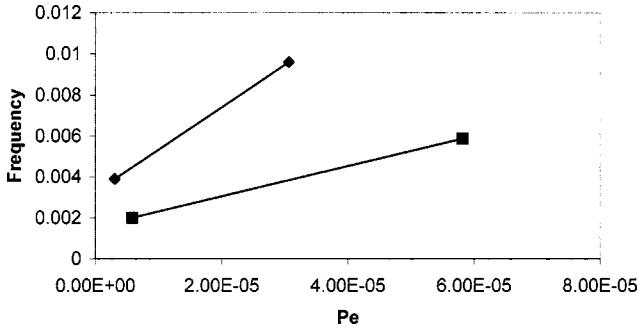

FIG. 8. The absolute value of the imaginary part of $\tilde{B}$, which is the dimensionless frequency, is plotted against Pe. The top curve is for $\phi=0.7$ and the bottom for $\phi=0.9$. Higher points are for $U=6.67$ and the lower points are for $U=10$. These are from reaction controlled region for the small $\tilde{B}$ approximation.

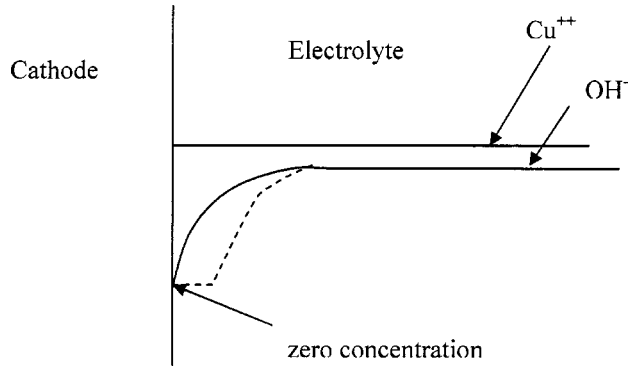

FIG. 9. The concentration profiles of the two reactive ions near the cathode. Cu^{++} is reaction controlled hence the concentrations are uniform, however, OH^- is diffusion controlled and the concentration falls to zero at cathode. One effect of perturbing the OH^- ion profile is shown; the concentration profile immediately surges forward.

not cover the middle range (of Pe and $\tilde{B}$) adequately. Nevertheless, the existence of these oscillations has been identified unambiguously. Most of these take place in the diffusion controlled regime. It should be pointed out that in the real parts of the complex roots, which are generally small, do not show a trend in signs, that is, they are positive or negative with almost equal probability, hence do not do much to clarify whether the oscillations are stable or unstable. Subsequently, oscillating systems will be referred to as stable for simplicity, although as stated earlier it cannot be ascertained whether they would grow or disappear except that in either case the rates will be small. The largest frequency calculated is only 0.001 Hz, when values of diffusivity D of 10^{-5} cm^2/s and $d=1$ mm are assumed, that is, two orders of magnitude smaller than in the experiments. They compare better if $d=0.1$ mm is assumed when the frequency increases to 0.01 Hz.

The experiments show that increasing current changes the frequency of the oscillations by only a small amount.[6] As seen in Fig. 7, changing values of U, and by extension changing current, does not change the frequency very significantly. Because of the numerical and the restricted nature of the results, it is not possible to check the effect of the boundary layer thickness d which is affected by stirring, on the oscillations. Experiments indicate that by varying stirring oscillations cannot be removed.[5] Experiments also indicate that the frequency of the oscillations is not very sensitive to pH changes. This is also reflected in the present results: If pH is increased, the bulk concentration c_{OH^-b} also increases. The manner in which the Damkohler number, D_{a2} is defined shows that it too increases with increasing c_{OH^-b} and pH. In Fig. 7, the points on the curve start on the left with D_{a2} of 179 and decrease to 2.18×10^{-18}, but the accompanying change in frequencies is hardly that significant.

As discussed earlier, one mechanism leading to the instability and formation of dendrites, has been given by Seshan.[9] At the tips of the dendrites, the diffusion lengths are lower and mass transfer is enhanced, which further increases the size of dendrites (Fig. 1). In contrast, the oscillations take place by a different mechanism. When the first reaction (copper formation) is reaction controlled, Cu^{++} ion concentration is almost uniform up to the cathode as shown in Fig. 9. However, the second reaction is diffusion controlled so that the concentration of OH^- ion falls to zero at the cathode as shown in the figure. If a disturbance occurs which sets back the OH^- ion concentration as shown with dashed line in the figure, then the second reaction stops, and only copper is deposited. However, the OH^- concentration gradient now is very large and OH^- ion concentration surges back to more than zero at the cathode. As the rates of second reaction are very large, D_{a2} is very large, mainly cuprous oxide is deposited at the cathode at this stage. But as D_{a2} is large, OH^- ions are again removed from this region, and the system continues to swing back and forth, and the main product swings from Cu to Cu_2O. These oscillations will not take place if D_{a2} is small because then the concentration of ions at cathode will not be zero, that is, not diffusion controlled. If D_{a2} is too large then the concentration of OH^- ions is held to zero at the cathode no matter what the disturbances may be. In general, the electrode reactions dissipate the electrical energy supplied to the cell. Formation of dendrites increases surface area and deposition rates. Thus, the instability that leads to formation of dendrites follows the natural law of increasing the rate of dissipation. When there are two reactions, the system favors one that gives rise to the larger dissipation. This growth is not unfettered as the supply of reactants is seriously depleted and the second reaction takes over, but is eventually superceded by the first reaction which promotes higher dissipation, etc.

Oscillations take place in the reaction controlled domain as well. Such oscillations are observed in the region of large ϕ. Thus, it is the first reaction which deposits copper that is more active. However, it is the second reaction which is dependent on the square of copper ion concentration which should be more active in this domain. Hence, a strong competition between the two can manifest itself in form of oscillations.

A very important difference between the results of slow mode studied by Seshan[9] and those of the fast mode studied here, should be emphasized. The dendrites predicted in the slow mode are irregularities that are seen as one travels on the face of the cathode. The fast mode results are valid for small wave numbers ω, and in fact are independent of wave

number ω. That is, as presented here, they are valid for only disturbances of infinite wavelengths. That means that they predict that no irregularities will be observed as one travels on the face of the cathode. However, traveling perpendicular to it would show periodically changing compositions. That is, the instability studied here is composition related. For a single reaction case, such as that studied by Seshan,[9] no new results are expected if the fast mode is analyzed. In the two reaction studied here, the results of slow mode analysis have not been included, but they do show the instability related to dendrite formation. Thus in the real system in cuprous oxide-copper system, composition of the deposit will alternate rapidly, and dendrites will grow very slowly alongside. It is now apparent that at later stages (beyond the linear analysis considered here), these two modes will be coupled, that is, the composition of deposited material will also vary periodically along the face of the cathode and even when the two reaction products are miscible.

When the reaction products are immiscible, the reaction products on the two surfaces will differ because the surface voltages and consequently the reaction rates differ. If, because of these differences, the oxide deposits at a lower rate on the oxide surface and the metal deposits at a lower rate on the metal surface, continued switchovers, that is, oscillations will occur. In other words, it is prompted by spatial variations in u_s on the electrode surface. One such scheme has been studied by Erie *et al.*[7] However, diffusion has not been included in their analysis, and reaction schemes which oscillate are generally very rare. When two materials deposited on the cathode, disturbances of some wave number ω_0, will be promoted. The corresponding wavelength $\lambda_0 = 2\pi/\omega_0$, represents a length scale describing segregation between copper-cuprous oxide on the surface of the cathode.

The main result here that the two-reaction system is capable of showing oscillations, is both in the physical mechanisms it brings into focus and for the clarifications on the elements of linear stability analysis needed to demonstrate their existence.

[1] E. W. Bohannan, L.-Y. Huang, F. S. Miller, M. G. Shumsky, and J. A. Switzer, Langmuir **15**, 813 (1999).
[2] J. A. Switzer, C.-J. Hung, L.-Y. Huang, E. R. Switzer, D. R. Kammler, T. D. Golden, and E. W. Bohannan, J. Am. Chem. Soc. **120**, 3530 (1998).
[3] Y. Zhou and J. A. Switzer, Scr. Mater. **38**, 1731 (1998).
[4] Y. C. Zhou and J. A. Switzer, Mater. Res. Innovations **2**, 22 (1998).
[5] J. A. Switzer, C. J. Hung, L.-Y. Huang, F. S. Miller, Y. C. Zhou, E. R. Raub, M. G. Shumsky, and E. W. Bohannan, J. Mater. Res. **13**, 909 (1998).
[6] L.-Y. Huang, E. W. Bohannan, C.-J. Hung, and J. A. Switzer, Isr. J. Chem. **37**, 297 (1997).
[7] B. H. Erné, F. Ozanam, M. Stchakovsky, D. Vanmaekelbergh, and J.-N. Chazalviel, J. Phys. Chem. B **104**, 5961 (2000); **104**, 5974 (2000).
[8] A. Iwamoto, T. Yoshinobu, and H. Iwasaki, Phys. Rev. Lett. **72**, 4025 (1994).
[9] P. K. A. Seshan, Ph.D. thesis, Chemical Engineering Department, Carnegie-Mellon University, Pittsburgh, PA, 1975.
[10] C. A. Miller and P. Neogi, *Interfacial Phenomena* (Marcel Dekker, New York, 1985), p. 240.
[11] C. A. Miller, in *Surface and Colloid Science*, edited by E. Matijevic (Plenum, New York, 1979), Vol. 10, p. 227.
[12] L. E. Johns and R. Narayanan, *Interfacial Instability* (Springer, New York, 2002), p. 244.
[13] M. Rosso, E. Chassaing, J.-N. Chazaviel, and T. Gordon, Electrochim. Acta **47**, 1267 (2002).
[14] W. W. Mullins and R. F. Sekerka, J. Appl. Phys. **35**, 444 (1964).
[15] E. J. W. Verwey and J. T. G. Overbeek, *Theory of Stability of Lyophobic Colloids* (Elsevier, Amsterdam, 1948), p. 27.
[16] T. K. Sherwood, R. L. Pigford, and C. R. White, *Mass Transfer* (McGraw-Hill, New York, 1975), p. 150.
[17] J. S. Newman, *Electrochemical Systems*, 2nd ed. (Prentice-Hall, Englewood Cliffs, NJ, 1991), pp. 180, 186.
[18] G. Prentice, *Electrochemical Engineering Principles* (Prentice-Hall, Englewood Cliffs, NJ, 1991), p. 93.
[19] S. C. Nam, S. H. Um, C. Y. Lee, Y. Tak, and C. W. Nam, Kongop Hwahak **8**, 645 (1997).